

# Wider Pore Superficially Porous Particles for Peptide Separations by HPLC

S.A. Schuster, B.M. Wagner, B.E. Boyes, and J.J. Kirkland

Advanced Materials Technology, Inc., 3521 Silverside Rd., Ste. 1-K, Quillen Bldg., Wilmington, DE 19810

## Abstract

Fused-core superficially porous particles have recently created considerable interest for high-performance liquid chromatography separations because of their unusual high column efficiency and much lower back pressure when compared to sub-2- $\mu\text{m}$  particles. With superficially porous particles, larger solutes can move rapidly in and out of a thin porous shell, resulting in reduced band broadening at higher mobile phase velocities for greater separation speeds. The original silica fused-core particles were 2.7  $\mu\text{m}$  in diameter with a 0.5- $\mu\text{m}$  thick shell of 90 Å pores designed for the fast separation of small molecules with molecular weights of less than approximately 5000. This manuscript describes new fused-core particles with similar physical characteristics except with a porous shell of 160 Å pores designed specifically for rapidly separating peptides (and some small proteins) with molecular weights up to approximately 15,000 Daltons. Because of the larger pore size, restricted diffusion of these larger molecules is not seen since ready access to the entire porous shell is featured. Data are given to define sample loading qualities for columns of these new particles. Column stability studies indicate that these particles bonded with a sterically protected  $\text{C}_{18}$  stationary phase can be used at low pH and higher temperatures with excellent results. The wider-pore particles of this study are shown to be particularly useful with a mass spectrometer detector for the rapid gradient separation of peptides using both volatile trifluoroacetic acid and formic acid containing mobile phases. Examples are provided for the separation of complex peptide mixtures to illustrate the capabilities for columns of these new wider-pore, fused-core particles.

## Introduction

Fused-core<sup>TM</sup> superficially porous silica particles with solid cores and porous outer shells have recently received considerable attention from the scientific community because of the unusual high efficiency and stability of these materials (1–7). Columns of these unique 2.7- $\mu\text{m}$  fused-core particles have shown separation efficiencies comparable to sub-2- $\mu\text{m}$  particles but at less than half the operating back pressure (5,8,9). This feature has resulted in very fast, robust separations with ordinary high-performance liquid chromatographic apparatus without the need for expensive very high pressure instruments (4,5,10).

With superficially porous particles, reduced band broadening occurs at higher mobile phase velocities compared to totally porous particles as solutes can rapidly move in and out of a thin porous outer shell for greater separation speed. The basic characteristics of superficially porous particles (there called pellicular particles) was first described by Horvath and Lipsky (11).

Previous commercially available fused-core particles with a porous shell of 90 Å pores were designed for the rapid separation of small molecules, typically materials with a molecular weight of approximately 5000 or less (2,5,12).

This presentation describes new fused-core particles with wider pores that are designed specifically for separating peptides and other molecules up to approximately 15,000 Daltons. These new particles retain the efficiency and stability of the original smaller-pore fused-core materials, but because of the wider pores, they allow a much wider range of molecular size for fast separations with gradients. Because of the thin porous shell, superficially porous particles exhibit more efficient separations of larger molecules, compared to totally porous particles, especially at higher mobile phase velocities. Unlike totally porous particles with longer flow-through pores, larger solutes with poor diffusional properties (e.g., large peptides and small proteins) can still rapidly enter the thin porous shell of fused-core particles, engage the stationary phase, and then quickly leave to resume the chromatographic process with minimal band broadening. This presentation describes the characteristics of the new wider-pore fused-core particles, including data on effect of pore size, sample loading, stability of  $\text{C}_{18}$ -bonded columns, and examples of separations for complex peptide mixtures.

## Experimental

Fused-core particles have been designed and prepared by Advanced Materials Technology, Inc., (Wilmington, DE). These high-purity Type B silica particles have an overall diameter of 2.7  $\mu\text{m}$ , with a solid core diameter of 1.7  $\mu\text{m}$  and an outer porous shell thickness of 0.5  $\mu\text{m}$ . The new wider-pore particles have an average pore diameter of 160 Å (BET), compared with 90 Å pores for the original Halo particles. The surface area of these new particles is  $\sim 80 \text{ m}^2/\text{g}$ , with a pore volume of  $\sim 0.30 \text{ mL/g}$  and an overall particle density of 1.3 cc/g. Columns of the wider-pore particles with 0.21–0.46 cm i.d. have been prepared by typical

\*Author to whom correspondence should be addressed: email jjackkirkland@att.net

slurry-packing methods with lengths ranging from 30–150 mm and are called Halo Peptide ES-C<sub>18</sub> columns. The C<sub>18</sub> bonded stationary phase was chosen for these particles to enhance retention of important smaller peptides that result when proteins undergo tryptic digestion. Totally porous 3- $\mu\text{m}$  ACE C<sub>18</sub> columns were obtained from Mac-Mod Analytical (Chadds Ford, PA). Chromatographic data have been obtained on these columns using an Agilent Model 1100 liquid chromatograph (Palo Alto, CA) with a 5- $\mu\text{L}$  semi-micro UV detector cell. Some experiments were also carried out with an Agilent Model 1200 instrument with a diode array detector. The column stability studies were performed with a Shimadzu Prominence liquid chromatograph (Kyoto, Japan).

The wider-pore fused-core particles were bonded with C<sub>18</sub> ligands to produce stationary phases of very high stability when operated with low pH mobile phases, even at higher temperatures. Silanes for these reactions were obtained from Gelest, Inc. (Morrisville, PA), and chemicals for mobile phases and other ordinary laboratory operations were obtained from VWR International (West Chester, PA). Polystyrene standards for size exclusion studies were obtained from Polymer Laboratories (Amherst, MA). Peptides and proteins used in these studies were obtained from Sigma Aldrich (St. Louis, MO), Promega (Madison WI), and AnaSpec (Freemont, CA). Surface area, pore size, and pore size distribution measurements were performed on a Micromeritics Instrument Corporation Tristar II BET instrument (Norcross, GA). Scanning electron microscopic measurements were performed by Micron, Inc. (Wilmington, DE).

Tryptic digests of apomyoglobin were prepared in this laboratory. Equine myoglobin was rendered free of the haem group by acid-acetone precipitation, followed by dialysis against 10 mM ammonium bicarbonate. The resulting apomyoglobin was denatured, diluted, and digested with modified trypsin (Promega) at a 1/40 enzyme to protein ratio. Digestions were terminated by adjusting the mixture to 1% with respect to acetic acid, followed by storage at  $-25^{\circ}\text{C}$ . Tryptic digest fragments were identified in eluates off column by fraction collection, drying in the Savant rotary vacuum system, dissolved in 0.1% TFA in water then were

infused into the Thermo Fisher (Waltham, MA) LTQ FT ion-trap mass spectrometer (University of Georgia, CCRC, Dr. Ron Orlando). The identities of tryptic fragments on the accompanying chromatograms were aligned to sequences of the Asn 104 variant of MYG\_HORSE (P68082). Peak capacities were calculated using single peptides of the digest mixture to assess peak widths, which were averaged together to generate a mean value for the separation. The expression used for this calculation was:

$$(t_G - t_i)/W$$

where  $t_G$  is the last measurable peak in the gradient,  $t_i$  is the first measurable peak in the gradient, and  $W$  is the 4-sigma width of these peaks.

The reported values are derived for this specific mixture of tryptic fragments and are a reasonable estimate of column peak capacities for complex mixtures.

Scanning electron micrographs (SEM) of the wider-pore fused-core particles are shown in Figure 1, and a cross-section electron micrograph of these same particles is in Figure 2. The latter micrograph clearly shows the solid core and porous shell structure of these fused-core particles. Figure 3 shows a comparison of BET pore size distribution plots for the original Halo C<sub>18</sub> fused-core particles with 90 Å pores and the new wider-pore Halo Peptide particles with 160 Å pores designed for separating pep-

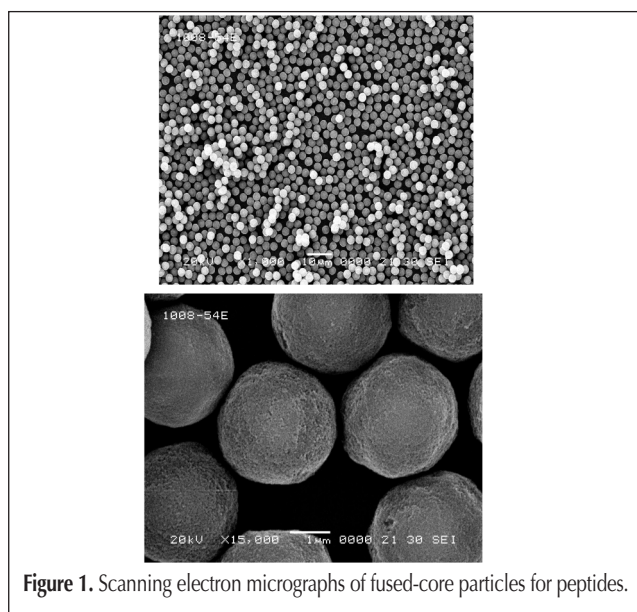


Figure 1. Scanning electron micrographs of fused-core particles for peptides.

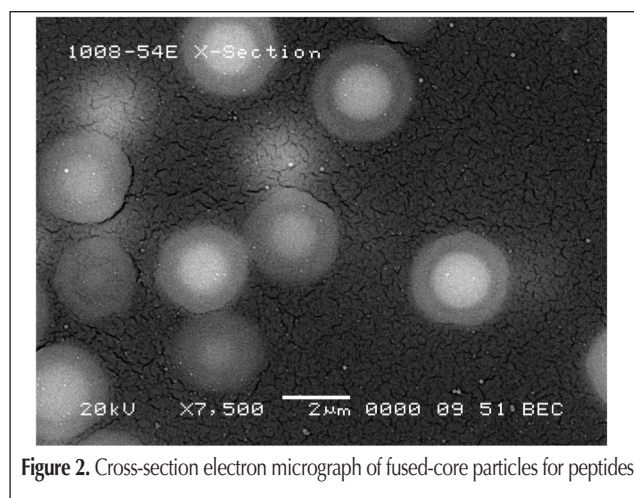


Figure 2. Cross-section electron micrograph of fused-core particles for peptides

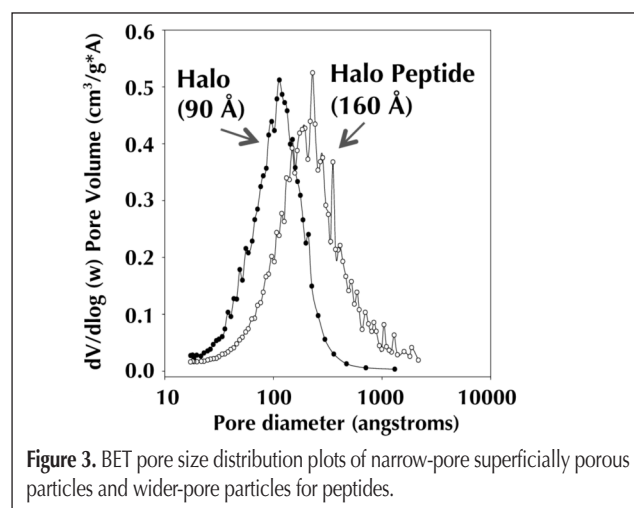


Figure 3. BET pore size distribution plots of narrow-pore superficially porous particles and wider-pore particles for peptides.

tides and small proteins. Size-exclusion chromatography plots performed on these two particles with polystyrene standards are shown in Figure 4. The wider pores of the new particles and the higher molecular weight range available are clearly defined in these plots, compared to data from narrower-pore fused-core Halo particles.

Data in some figures were fitted using the Knox equation, a variation of the classical van Deemter relationship,

$$h = A v^{1/3} + B/v + C v \quad \text{Eq. 1}$$

where  $h$  = reduced plate height (plate height/particle size),  $v$  = mobile phase velocity, and  $A$ ,  $B$ ,  $C$  are column constants representing eddy diffusion, longitudinal mass transfer, and mobile phase plus stationary phase mass transfer, respectively. (13).

## Results and Discussion

### Comparison to original fused-core particles

Columns of both original fused-core (Halo-C<sub>18</sub>) and the wider-pore fused-core (Halo Peptide ES-C<sub>18</sub>) particles show essentially identical efficiency for small neutral compounds, as illustrated in

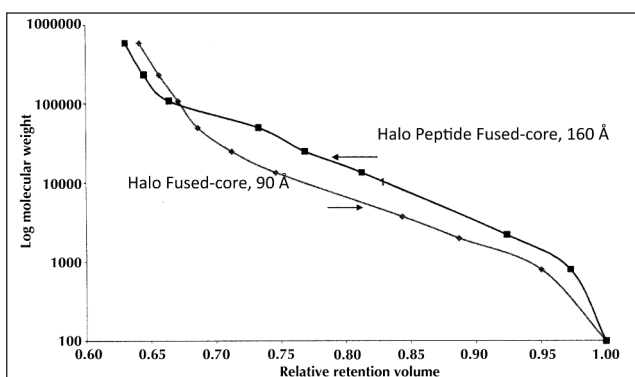


**Figure 4.** Size-exclusion chromatography comparison of fused-core silica particles. Columns: 4.6 × 150 mm silica; Sample: polystyrene standards; Mobile phase flow rate: 1.0 mL/min; Detection: UV, 254 nm.

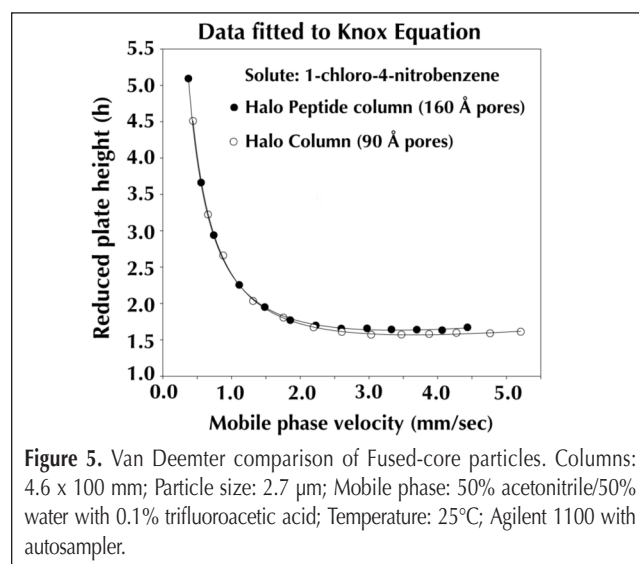


**Figure 5.** Van Deemter comparison of Fused-core particles. Columns: 4.6 × 100 mm; Particle size: 2.7 μm; Mobile phase: 50% acetonitrile/50% water with 0.1% trifluoroacetic acid; Temperature: 25°C; Agilent 1100 with autosampler.

Figure 5. Data were obtained on a commercial instrument using an autosampler with no corrections for extra-column effects. These results were expected because the particle size and porous shell thickness were essentially identical for the two particles (e.g., Halo: 2.82 μm, standard deviation, 0.14 μm; Halo Peptide: 2.85 μm, standard deviation, 0.14 μm).

Gradient separations of a mixture of peptides and small proteins are compared in Figure 6 for the fused-core narrow-pore (Halo-C<sub>18</sub>) and the wider-pore fused-core (Halo Peptide ES-C<sub>18</sub>) particles. The smaller peptides in Figure 6A show essentially equivalent peak half-widths and peak shapes for the two columns. However, small proteins of higher molecular weight (ribonuclease, peak 6 and insulin, peak 7) show wider peak widths for the smaller-pore particles, suggesting some restricted diffusion that is not a feature of the wider-pore particles. The slight selectivity differences in these two chromatograms are largely due to the fact that the two columns have slightly different C<sub>18</sub> stationary phases. Peak widths for the wider-pore par-

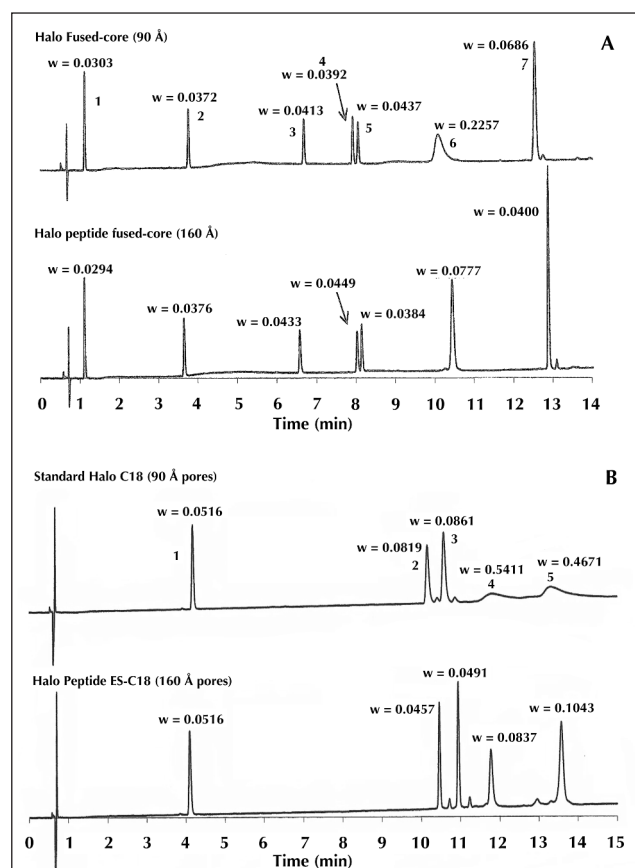


**Figure 6.** Comparison of half-height peak widths for fused-core particles. Columns: 4.6 × 100 mm; Temperature: 30°C; samples dissolved in mobile phase A. The y-axis represents relative absorbance for UV detection at 220 nm.

**Part A:** Peptides, peak numbers are as follows: 1, Gly-Tyr; 2, Val-Tyr-Val; 3, Met Enkephalin; 4, Angiotensin II; 5, Leu-Enkephalin; 6, bovine ribonuclease; 7, insulin. Mobile phase A: 10% acetonitrile–0.1% trifluoroacetic acid; Mobile phase B: 70% acetonitrile–30% water–0.1% trifluoroacetic acid; gradient: 0% B to 50% B in 15 min; flow rate: 1.5 mL/min; detection: 220 nm.

**Part B:** Peptides, Small proteins, peak numbers are as follows: 1, Enk-Leu; 2, bovine insulin; 3, human insulin; 4, cytochrome C; 5, lysozyme; Mobile phases same as in 6A; gradient: 15% B to 50% B in 15 min; Other conditions as in 6A.



ticles with all molecules in this mixture are essentially equivalent, indicating that the wider pore diameter now allows easy access for all of these probes without any restricted diffusion. In Figure 6B, the lack of restricted diffusion is clearly seen for small proteins (cytochrome C and lysozyme, peaks 4 and 5, respectively) for the wider pore particles, compared to the fused-core Halo column with smaller pore particles.

### Comparison with totally porous particles

Figure 7 compares van Deemter plots for the beta amyloid fragment 1–38 (MW = 4100) using a high-quality 3- $\mu\text{m}$ ,

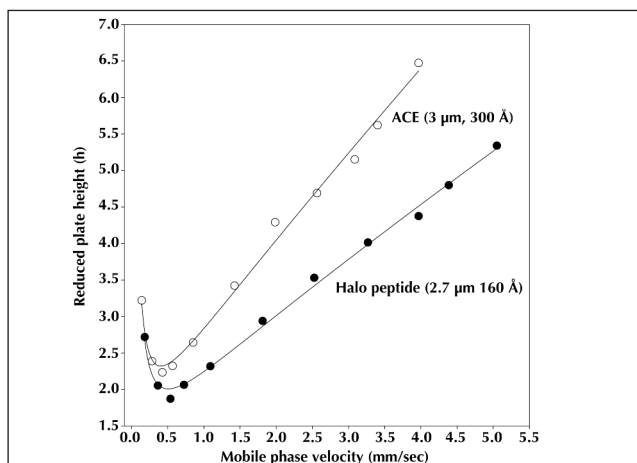


**Figure 7.** Van Deemter plots for columns of fused-core particles and totally porous particles. Columns: 4.6  $\times$  100 mm Halo Peptide ES-C<sub>18</sub>, 2.7  $\mu\text{m}$  and 4.6  $\times$  100 mm ACE C<sub>18</sub>, 3  $\mu\text{m}$ ; Mobile phase for Halo Peptide: 29% acetonitrile–71% water–0.1% trifluoroacetic acid; Mobile phase for ACE: 28% acetonitrile–72% water–0.1% trifluoroacetic acid; Temperature: 60°C; Sample: beta amyloid 1–38 (MW = 4100); Agilent 1100 with autosampler.

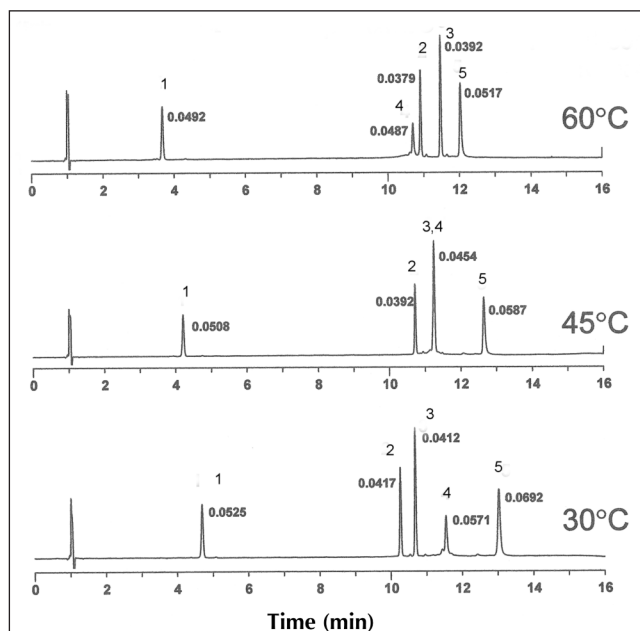


**Figure 8.** Effect of temperature on separation of small proteins. Column: 4.6  $\times$  100 mm fused-core for peptides; Conditions same as in Figure 6B, except flow rate: 1.0 mL/min. The y-axis represents relative absorption for UV detection at 220 nm.

300  $\text{Å}$  totally porous particle (ACE) and the new 2.7- $\mu\text{m}$  Halo Peptide 160  $\text{Å}$  fused-core particle. Compared to totally porous particles, the smaller increase in plate height for the fused-core particles with increased mobile phase velocity is an indication of superior mass transfer (e.g., smaller van Deemter C-term) for the superficially porous particles. Even though the ACE particles had 300  $\text{Å}$  pores compared to the 160  $\text{Å}$  pore size for the Halo Peptide particles, the latter material still exhibits superior mass transfer properties. Superficially porous fused-core particles have mass transfer advantages for separations of larger molecules. Larger molecules with poorer diffusion properties do not have easy access to the deeper pores present in totally porous particles at higher mobile phase velocities. With superficially porous particles, molecules can move rapidly in and out of the thin porous shell to result in less band broadening and higher separation speed with lower loss in separation efficiency and resolution.

### Effect of increased temperature operation

In keeping with other studies (14,15), increased column efficiency for columns of the wider pore particles can be gained by operating columns at increased temperature, as illustrated in Figure 8. Here, band widths are decreased at higher temperatures for more efficient separations, which also predict better resolution and higher peak capacities at higher operating temperatures. Therefore, operation at higher temperatures (e.g., 60°C) can be effective and should be considered for separating peptides and some small proteins. As also indicated in Figure 8, changes in temperature also can result in band spacing (selectivity) changes, which may be useful or detrimental depending on the specific sample separated.

### Column stability

The C<sub>18</sub> stationary phase used on the new wider-pore fused-core particles provides excellent column stability at low pH and higher temperatures. This stability is documented by the plots in Figure 9, where wider-pore C<sub>18</sub> columns were used to successively gradient-separate a mixture of a peptide and a small protein using a mobile phase of acetonitrile and 0.1% trifluoroacetic

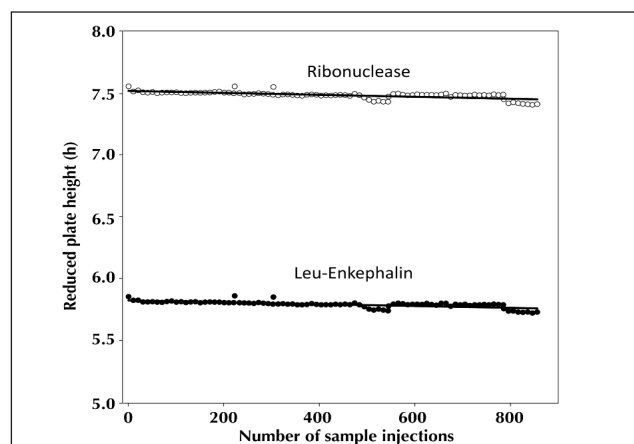


**Figure 9.** Stability of fused-core columns (retention time vs. number of injections). Column: 2.1  $\times$  100 mm Halo Peptide ES-C<sub>18</sub>; Mobile phase A: water–0.1% trifluoroacetic acid; Mobile phase B: 70% acetonitrile–0.1% trifluoroacetic acid; Gradient: 9–55% B in 10 min; Flow rate: 0.5 mL/min; Temperature: 60°C.

acid (pH < 2) at 60°C. After more than 850 injections (~ 10,000 column volumes) of this gradient mobile phase at 60°C, retention times and peaks widths (not shown here) remain essentially constant for these test compounds.

### Sample loading

Because of the relatively high surface area of the wider-pore superficially porous particles (~ 80 m<sup>2</sup>/g), sample loading properties for this material are quite adequate for most applications, as shown in Figure 10. Little change in column efficiency is seen up until at least 1 µg of the small protein, insulin. For the nar-

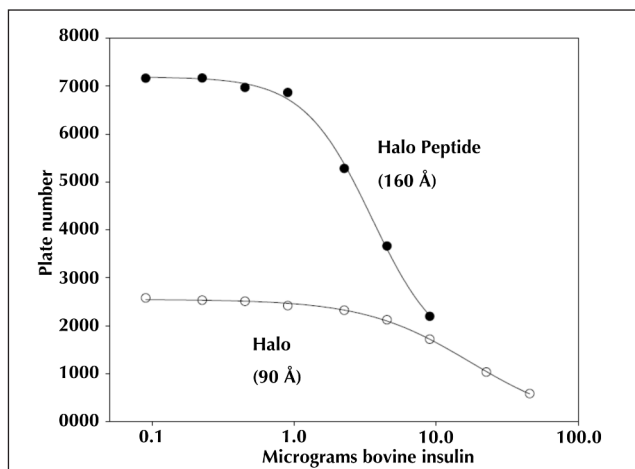


**Figure 10.** Effect of sample loading on peptide fused-core column. Sample: bovine insulin, MW = 5733; Columns: 4.6 × 100 mm; Mobile phase: 31.5% acetonitrile/68.5% 0.1% trifluoroacetic acid; Temperature: 60°C; Sample volume: 10 µL.

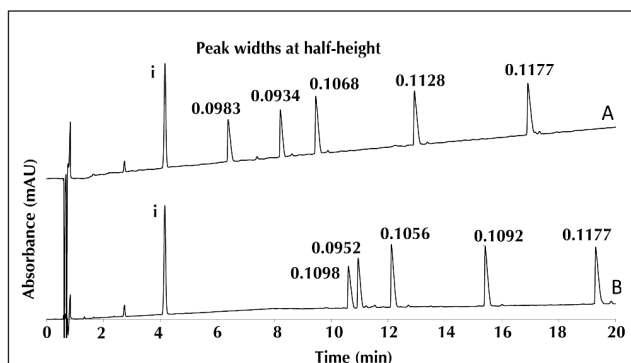


**Figure 11.** Peptide separations for fused-core column with acidic mobile phases. Columns: 4.6 × 100 mm, Halo Peptide ES<sub>18</sub>; Gradient: 5% B to 25% B in 20 min; flow rate: 1.5 mL/min; temperature: 60°C; detection: 210 nm; Sample: S1-S5 -Peptide Retention Standard containing 5 C-terminal amide decapeptides denoted S1S5 having the generic formula Ac-Arg-Gly-X-X-Gly-Leu-Gly-Leu-Gly-Lys-Amide. Four of these peptides are Na-acetylated with the sequence variation: Gly3-Gly4, Ala3-Gly4, Val3-Gly4, Val3-Val4. The fifth peptide, Ala3-Gly4 contains a free Na-amino group. The y-axis represents relative absorbance values for UV detection at 210 nm.

**Part A:** Formic acid method: Mobile phase A: water–0.1% formic acid–20 mM ammonium formate; Mobile phase B: 80% acetonitrile–0.1% formic acid–20 mM ammonium formate

**Part B:** Trifluoroacetic acid method: Mobile phase A: water–0.1% trifluoroacetic acid; Mobile phase B: 80% acetonitrile–20% water–0.1% trifluoroacetic acid

rower-pore fused-core (Halo) column, the same protein results in about a three-fold decrease in plate number even at the smallest sample size studied. This effect suggests restricted diffusion for this protein within the smaller pores of the particles. These results indicate that relatively large sample loadings can be used with the wider-pore fused-core particles for the detection of trace compounds in complex mixtures.

### Mobile phase effects

The wider-pore particles of the present study are particularly suited for using the mass spectrometer (MS) as a detector for gradient separations of peptides and small proteins. This is illustrated in Figure 11, which shows comparative peptide and small protein separations using volatile trifluoroacetic acid (TFA) and formic acid (FA) mobile phases. Separations using formic acid containing mobile phases are sometimes preferred for MS detection of peptides because the ionization efficiency with these materials is much higher, permitting better detection of minor components (16). As shown in Figure 11, peak shape and peak width are comparable for the two mobile phases. Retention is higher for the test mixture in the TFA mobile phase, presumably because of the tendency of TFA to form ion-pairs that result in greater retention. Formic acid has a much lower tendency for ion-pair formation.

### Separation of complex peptide mixtures

The usefulness of the wider-pore particles for separating complex mixtures of peptides is illustrated in Figure 12 for the separation of an apomyoglobin digest. The separation with a 100 mm column in the upper trace generates a peak capacity of approximately 216 for this 60 min gradient separation. Because this column showed a back pressure of only 240 bar under the conditions used, it was possible to connect another 100 mm column of the same type (total of 200 mm) to carry out the separation shown in the bottom trace. This 120 min gradient separation was performed at 476 bar and generated a peak capacity of approximately 297, resulting in much-improved resolution of components in the digest, including overlapping peaks.

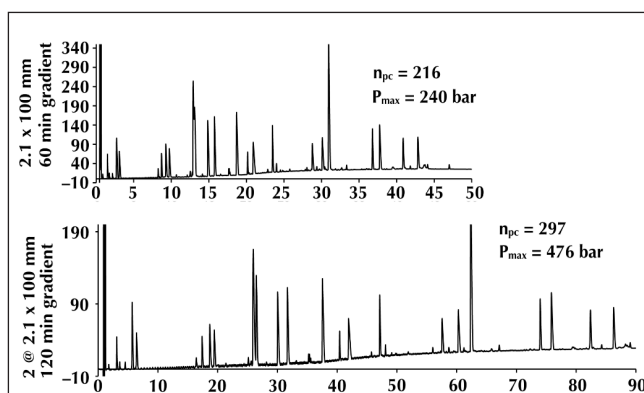


**Figure 12.** Gradient separation of apomyoglobin digest. Conditions; Columns: 2.1 × 100 mm; Mobile phase A: water–0.1% trifluoroacetic acid; Mobile phase B: 80% acetonitrile–20% water–0.1% trifluoroacetic acid; Gradients as shown; Flow rate: 0.5 mL/min; Temperature: 45°C; Injection volume: 15 µL (15 µg); The y-axis represents relative absorbance values for detection at 210 nm.

## Conclusions

New wider-pore fused-core superficially porous silica particles have been prepared for the fast separation of peptides and small proteins. The pore size of these particles allow the rapid separation of such materials with sizes up to approximately 15,000 Daltons without evidence of restricted diffusion limiting column efficiency and separation resolution. The unusually high column efficiency of Halo fused-core columns is maintained by columns of the new wider pore particles primarily due to the very narrow particle size distribution and the higher particle density of these materials. The stationary phase used on these particles is highly stable to both low pH and higher temperatures. Sample loading properties are generous for these particles because of the effective surface area. Both trifluoroacetic acid and formic acid mobile phases can be used effectively with the new particles with comparable efficiency and peak shapes. The new wider-pore particles are especially suited for rapidly separating complex protein digest mixtures, especially at higher operating temperatures for superior efficiency.

## Acknowledgments

The authors greatly appreciate the mass spectrometer peptide identifications by Dr. Ron Orlando, University of Georgia, CCRC USA, and the size-exclusion measurements performed by Dr. J.J. DeStefano, Advanced Materials Technology, Inc., Wilmington DE.

## References

1. N. Marchetti, A. Cavazzini, F. Gritti, and G. Guiochon. Gradient elution separation and peak capacity of columns packed with porous shell stationary phases. *J. Chromatogr. A* **604**: 203–211 (2007).
2. J.J. Kirkland, T.J. Langlois, and J.J. DeStefano. Fused-core particles for HPLC columns. *American Lab.* **39**: 18–21 (2007).
3. D.V. McCalley. Evaluation of the properties of a superficially porous

- silica stationary phase in hydrophilic interaction chromatography. *J. Chromatogr. A* **1193**: 85–91 (2008).
4. J.J. Salisbury. Fused-core particles: A Practical alternative to sub-2 micron particles. *J. Chromatogr. Sci.* **46**: 883–886 (2008).
5. J.J. DeStefano, T.J. Langlois, and J.J. Kirkland. Characteristics of superficially porous particles for fast HPLC: Some performance comparisons with sub-2 micron particles. *J. Chromatogr. Sci.* **46**: 354–260 (2008).
6. S. Fekete, J. Fekete, and K. Ganzler. Shell and small particles: Evaluation of new column technology. *J. Pharma. Biomed. Anal.* **49**: 64–71 (2009).
7. Y. Zhang, X. Wang, P. Mukherjee, and P. Petersson. Critical comparison of performances of superficially porous and sub-2  $\mu\text{m}$  particles under optimized ultra-high pressure conditions. *J. Chromatogr. A* **1216**: 4597–4605 (2009).
8. J.M. Cunliffe and T.D. Maloney. Fused-core particle technology as an alternative to sub-2  $\mu\text{m}$  particles to achieve high separation efficiency with low back pressure. *J. Separ. Sci.* Published online Nov. **14**: 3104–3109 (2007).
9. S. Fekete, J. Fekete, and K. Ganzler. Characterization of new types of stationary phases for fast liquid chromatographic applications. *J. Pharma. Biomed. Anal.* **50**: 703–709 (2009).
10. Y. Hsieh, C.J.G. Duncan, and J.M. Brisson. Fused-core Silica column High-performance liquid chromatography/tandem mass spectrometric determination of rimonabant in mouse plasma. *Anal. Chem.* **79**: 5668–5673 (2007).
11. C.G. Horvath and S.R. Lipsky. Rapid analysis of ribonucleosides and bases at the picomole level using pellicular cation exchange resin in narrow bore columns. *Anal. Chem.* **41**: 1227 (1969).
12. N. Marchetti and G. Guiochon, High peak capacity separations of peptides in reversed-phase gradient elution liquid chromatography on columns packed with porous shell particles. *J. Chromatogr. A* **1176**: 206–216 (2007).
13. L.R. Snyder, J.J. Kirkland, and J.W. Dolan. *Introduction to Modern Liquid Chromatography*, 3<sup>rd</sup> ed., John Wiley and Sons, Hoboken, NJ, (2009), P. 43.
14. H. Chen and C. Horvath. High-speed, high-performance liquid chromatography of peptides and proteins. *J. Chromatogr. A* **705**: 3–20 (1995).
15. B.E. Boyes and J.J. Kirkland. Rapid high-resolution HPLC separation of peptides using small particles at elevated temperatures. *Peptide Res.* **6**: 249–258 (1993).
16. S. Zhou and M. Hamburger. *Rapid Comm. Mass Spec.* **9**: 1516–1521 (1995).

Manuscript received January 19, 2010;  
revision received March 23, 2010